Level Set for Semantic Segmentation with Edge Compensation

Zhipeng Lei[1], Wei Zheng[1], Yongxin Miao[1] and Xuan Fei[1*]

[1]Yingkou Electric Power Supply Company, State Grid Liaoning Electric Power Supply Co., Ltd., Kuandian, Liaoning, 118200, China

[*]Corresponding author's e-mail: litianjie_123@126.com

Abstract. This paper demonstrated that active contour based on points evolution is not suitable for Objects with blurring boundary segmentation. In irregular areas adjacent points have similar motion trends trapped into 'piles phenomena'. Level set should be preferred in practice. Whereas, classic level set lacks of perception in distance especially narrow and abnormal region. Consequently, we reported an algorithm localized level set that is able to improve accuracy. Meanwhile, in cases lost boundary of bone, we gave a strategy called edge compensation. Depending on shapes of neighborhood slices, defective section is estimated and restored effectively. Our experiments showed that the algorithm localized level set increases segmental quality with precision 99.74%. Additionally, it could not only rectify mistakes brought by incorrect initialization but also have a robust performance to overcome local region with highly inhomogeneous intensity.

1.Introduction

Semantic image segmentation is the process of turning an input image into a raster map, by assigning every pixel to an object class from a predefined class nomenclature. Automatic semantic segmentation has been a fundamental problem of remote sensing data analysis for many years [1-3]. In recent years there has been a growing interest to perform semantic segmentation also in urban areas, using conventional aerial images or even image data recorded from low-flying drones. Images at such high resolution (GSD 5–30 cm) have quite different properties. Intricate spatial details emerge like for instance road markings, roof tiles or individual branches of trees, which increase the spectral variability within an object class. The spectral resolution of sensors is limited to three or four broad bands so spectral material signatures are less distinctive. Hence, a large portion of the semantic information is encoded in the image texture rather than the individual pixel intensities, and much effort has gone into extracting features from the raw images that make the class information explicit.

Manual segmentation slice by slice costs unacceptable amount of time, nearly 8-10 hours per image [10]. Semi-automatic or fully automatic methods are necessary as soon as possible. Few features influence fully automatic methods negatively [11]. Therefore, researchers pay more attentions on interactive segmentations like random walk [12], active contour [13], level set [14] and etc. Relying on initial mark, result shows more attractive and stable. This paper mainly focuses on segmentation of **Objects with blurring boundary**.

In segmentation of Objects with blurring boundary, relatively smaller number of papers are published. Some difficulties lead to: 1. great variations of Objects with blurring boundary anatomy in individual; 2. irregularity of Objects with blurring boundary boundary; 3. extreme inhomogeneity of

intensity inside cavity; 4. lost boundary destroyed by tumor. Most of papers only report their progress under fine condition of Objects with blurring boundary. In fact, they cannot be carried out in clinics.

[15, 16] presented algorithms based on thresholding of extracting bones. Great variation of intensity makes it impossible to get an ideal result. Same problem comes into others for Objects with blurring boundary like region growing [17, 18, 19, 20, 21, 22]. [23] designed anisotropic localized active contour to refine coarse segmentation. For increasing significant features, some papers proposed to set up a statistical volumetric model as reference by PCA analysis. [24, 25, 26] combined the statistical shape into active contour process. Shape information was regarded as the crucial consideration of decision how to evolve. However, great changes of anatomical structure lead to undesirable results. Besides, with experiment and mathematical deduction we proved active contour based on points evolution runs incompetent within Objects with blurring boundary. Related details will be discussed later.

Localized level set method was reported in this study, which derives from real curve evolution and avoids 'piles'. Furthermore, localized level set was adopted for refinement after coarse segmentation, as if extra longer antennas would help to detect larger and interesting local regions. At last, we submitted an edge compensation strategy, in case when part of boundary is destroyed by tumor [27]. On evaluations, it was proved that our proposed method obviously has superior performances under possible conditions of Objects with blurring boundary.

2.Localized level set

For more accuracy, a refinement strategy is required. set up a model with distance regularization ([20]) - ([22]):

$$\varepsilon(\phi) = \mu R_p(\phi) + \lambda L_g(\phi) + \alpha A_g(\phi) \tag{1}$$

$$L_g(\phi) \triangleq \int_\Omega g\, \delta(\phi)|\nabla\phi| d\mathbf{X} \tag{2}$$

$$A_g(\phi) \triangleq \int_\Omega g\, H(-\phi) d\mathbf{X} \tag{3}$$

where ([22]) considers global region and speeds process of walking toward boundary. However, there is a restriction in ([20]). When zero level set locates in narrow and irregular area, it has difficulty to arrive in the boundary of long distance. ([21]) runs inside a only 8-neighborhood, as a result curve has been attracted by edge nearby at first. In order to resolve this trouble, we introduced localized level set method ([23]) that takes global and local region information into account simultaneously, which assists zero level set to escape from trapped area and improves accuracy.

$$\varepsilon(\phi) = \mu R_p(\phi) + \lambda L_g(\phi) + \beta B_g(\phi)$$

$B_g(\phi)$ describes difference between a point's interior and exterior. It looks like Chen-Vase model, but ([23]) refers sum of every point's $B_g(\phi)$ on curve. Here we ignore item $A_g(\phi)$ ([20]), since refinement has no demand for accelerating. To build a point's local interior or exterior we have a reference by:

$$Region(x, y) = \begin{cases} 1, & \|x - y\| \le r \\ 0, & otherwise \end{cases}$$

If y point is within radius r centered at x, we believe y locates in region of x. A point's interior contains the part of ball region inside its curve, exterior vice versa. Localized level set based on follows gradient flow:

$$\frac{\partial \phi}{\partial t} = \mu[\triangle \phi - div(\frac{\nabla \phi}{|\nabla \phi|})] + \lambda \delta(\phi) div(g \frac{\nabla \phi}{|\nabla \phi|}) + \beta \delta \phi(x) \int_{\Omega_y} R\,egion(x,y) \delta \phi(y) \cdot (\frac{(I(y) - u_x)^2}{A_u} - \frac{(I(y) - v_x)^2}{A_v}) dy$$

where u_x and v_x indicate a point's mean intensity of local interior and exterior respectively. A_u and A_v give areas of one point's interior and exterior by:

$$A_u = \int_{\Omega_y} R\,egion(x,y) \cdot H_\phi(y) dy$$

$$A_v = \int_{\Omega_y} R\,egion(x,y) \cdot (1 - H_\phi(y)) dy$$

With ([26]), minimum of ([23]) is obtained when interior and exterior of every point have maximum difference as far as possible. Experiments showed that localized level set cannot only give a improvement for irregular boundary, but hold a ability to repair faults resulting from incorrect initialization. What proved more excited is that it enables curve to jump out of areas with highly inhomogeneous intensity. In contrast, traditional solution lived on regulating coefficients.

3.Edge compensation

In usual, clinicians face massive sets of slices with tumor or related diseases. In visualization, they cause intensity shake tremendously which invokes sheltered boundary frequently, illustrated in Fig. 1. Definitely, lack of edge indicator leads to failed segmentation seriously, seen in Fig .1. For improvement, we proposed a novel strategy edge compensation capable of repairing lost edges in Objects with blurring boundary.

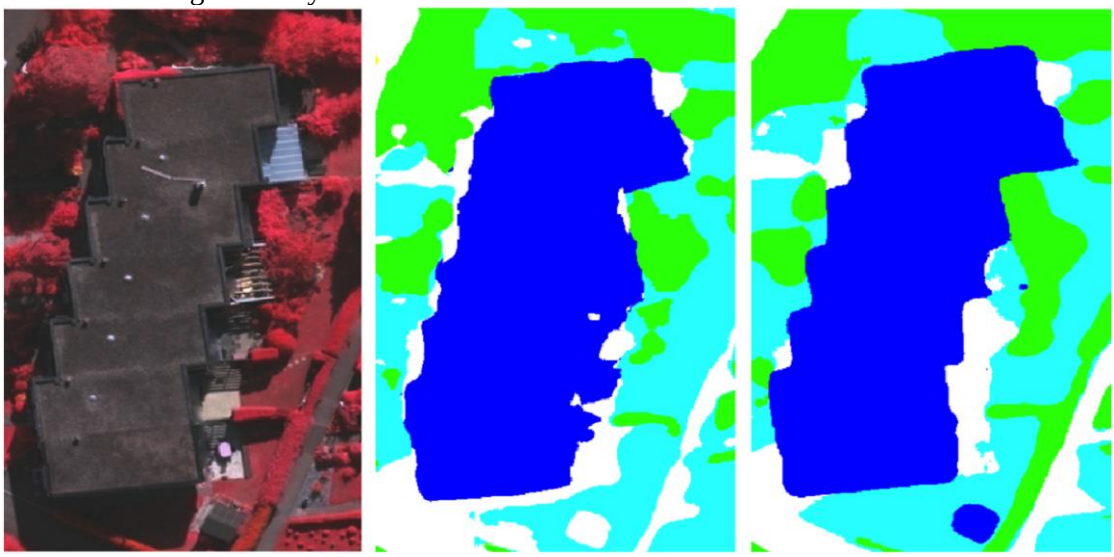

Figure 1. Objects with blurring boundary with sheltered boundary

Low rank gets used to describe row or column vectors correlation and more popular recently in image processing, for example matrix completion, robust PCA moving detection, and etc. In our research, we give a vector

$$\{x_1 \quad \cdots \quad x_n \quad y_1 \quad \cdots \quad y_n\}$$

to express shape of a curve C_n. If matrix $\{C_1 \quad C_2 \quad \cdots \quad C_n\}^T$ has a low rank, this group of curves is provided with a similar shape. imported this idea to reshape noisy ultrasound image. To incomplete Objects with blurring boundary, edge compensation depends on regularizing localized level set ([23]) with nuclear norm:

$$\min_{\mathbf{X}} F(\mathbf{X}) + \lambda R(\mathbf{X})$$

where $F(\mathbf{X})$ is a functional ([23]) and $R(\mathbf{X})$ corresponds to a convex but nonsmooth penalty of shapes nuclear norm. In convention, nonsmooth results in infeasible optimization. However, if $F(\mathbf{X})$ is differentiable with Lipschitz continuous gradient, the objective could be transformed as another form:

$$\mathbf{Q}_u(\mathbf{X}, \mathbf{X}') = \frac{\mu}{2}\left\|\mathbf{X} - \left[\mathbf{X}' - \frac{1}{\mu}\nabla\mathbf{F}(\mathbf{X}')\right]\right\|_F^2 + \lambda R(\mathbf{X})$$

([30]) is an approximation for ([29]) with a quadratic polynomial in local domain, which seems interpreted as a kind of Taylor series expansion. Therefore, we are able to find minimum locally. By iterations, the first item in ([29]) could be resolved easily. Accordingly, objective has been changed to another problem:

$$\min_{\mathbf{X}} \frac{1}{2}\|\mathbf{X} - \mathbf{Z}\|_F^2 + \frac{\lambda}{\mu}\|\mathbf{X}\|_*$$

where $\mathbf{Z} = \mathbf{X}^k - \frac{1}{\mu}\nabla\mathbf{F}(\mathbf{X}^k)$. introduced a singular value thresholding operator ([33]) to update ([32]) followed by

$$\mathbf{D}_\alpha(\mathbf{Z}) = \sum_{min(m,n)}^{i=1} (\sigma_i - \alpha)_+ \mathbf{u_i} \mathbf{v_i}^T$$

$$\mathbf{X}^{k+1} = \mathbf{D}_{\frac{\lambda}{\mu}}(\mathbf{X}^k - \frac{1}{\mu}\nabla F(\mathbf{X}^k))$$

$\mathbf{u_i}$ and $\mathbf{v_i}$ are left and right singular vectors of $\mathbf{Z}$, and ([34]) is the update rule of ([29]). In practice, we require neighborhood slices clear boundaries, which give edge compensation a powerful reference.

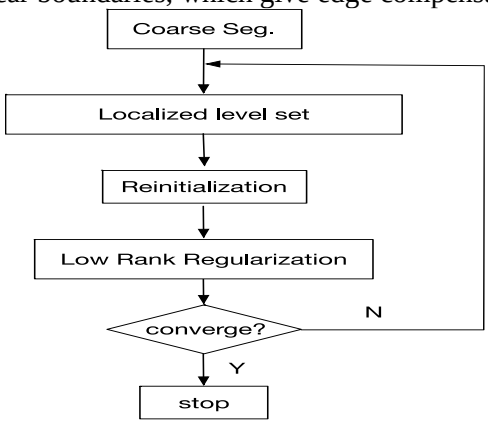

Figure 2. Procedure of edge compensation in refinement after Level Set evolution

4. Results and discussion

4.1 Evaluation measure

The manual segmentations of the Objects with blurring boundary were performed by five clinicians with more than 8 year experience. There is a quantitative evaluation for performance, which contains dice coefficient (DC), precision, recall and F-score four indexes. All of them depend on four

coefficients: true-positive (TP), false-positive (FP), true-negative (TN) and false-negative(FN). Certainly, we wish that methods would have low FP and FN. Higher DC, precision, recall and F-score mean a wonderful performance.

4.2 Evaluation of localized level set in refinement

We introduced algorithms to join our evaluation for comparison with our proposed method. specialized in segmentation of Objects with blurring boundary recently and are classic representatives in medical image segmentation.

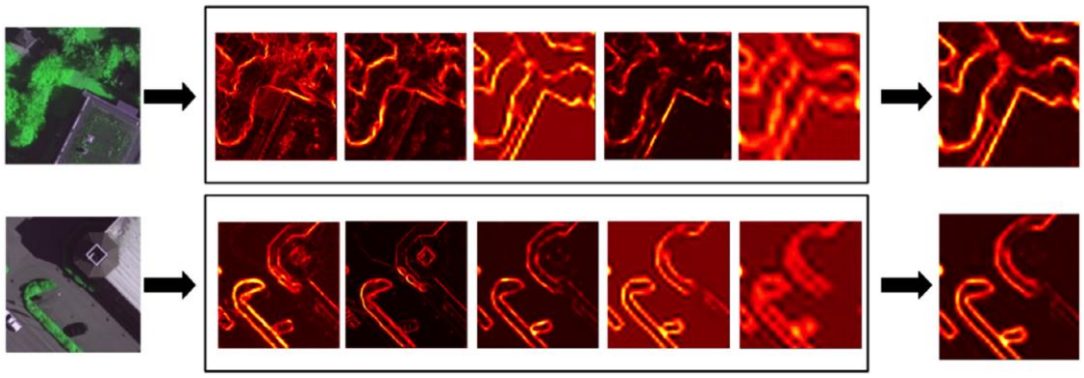

Figure 3. Results of level set with or without localized feature

It is known that plenty of Objects with blurring boundary are filled with pus or tumor Fig. 6(a). In visualization, intensity inside cavity is no longer close to zero but presents inhomogeneous. Although boundary is clear, there are gradient blurring disturbances so that traditional methods may stop far away Fig. 3. If we adjust control coefficients, it is possible to resolve this problem in certain image. However, inhomogeneity runs stochastic, and same parameters never sail all the time. Encouraged grows that localized level set succeeds to jump out of influenced area when considering distributions of gray in distance, shown in Fig. 6(c). have an important prerequisite: deformable registration. But varied intensity has to bring a incredible one. In part points of curve tend to be caught inside blurring region of high gradient and usually cause errors. Fig. 6(c) illustrates a case of proposed method.

At last, localized level set is also able to rectify faults brought by incorrect initial contour. Objects with blurring boundary segmentation serves 3D reconstruction for pre-surgical plan or FESS real-time location. Initial contour slice by slice with hands is too cumbersome. Automatic generation consults manual initializations on fore-and-aft slices. Sometimes because of abnormal variation, it probably provides incorrect estimation, so that they may be dragged by objects nearby or stand still In this situation, localized level set can repair overflowed segmentation as what we wish. Though it has similar effects, character of evolution on points indicates a low performance.

In metrics of recall, as the defect of curve evolution based on points, Chan-Vese, and performed not very well. Better cases belonged to owing to priori knowledge of shape, where it believed some areas should be what they wanted. Unfortunately, fault judgments frequently resulted in low precision or F-score. Nevertheless, our method focuses both 'global' and 'local' region. When quickly approaches edge, it makes efforts of refinement in neighbor area and acquires an acceptable segmentation. Radius of local region r plays an important role. As mentioned, it has three great potentials. In aspect of a larger r, ([26]) considers distant gradient to decide how to evolve. However, overlarge radius provides redundant information out of valid surroundings. In fact, a smaller r is able to modify overflowed curve. When error points near edge start to be drawn, subsequent points follow previous ones' motion. A butterfly effect happens. But smaller one can not help other two destinations. Figure. [radius] shows r impactions on three objectives. For every target we took 20 subjects in experiments with different r. Their performances were evaluated by F-score. According to three indicators, we preferred 20 as r at last.

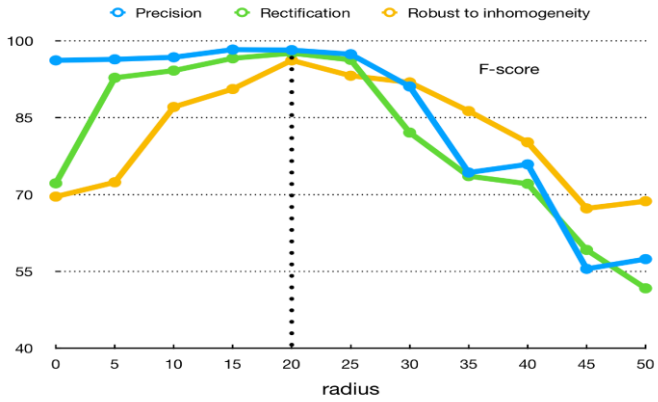

Figure 4. Effect of r in performance. Quantitative evaluation was done under three objectives: precision, rectification of incorrect initialization and inhomogeneous intensity. Evaluated standard selects F-score.

Objects with blurring boundary lose part of boundary by tumor intervention that causes failed segmentation. We have discussed this phenomena in Fig. 9. With edge compensation algorithm, references of neighborhood shapes provide a shortcut to restore. Figure.[com] is one of experiments and edge compensation strictly complies with rule proposed in Fig. 9.

5. Conclusion

This paper contributes several works to Objects with blurring boundary segmentation. At first, we demonstrate active contour based on points evolution cannot be suitable in irregular region. Level set should be preferred at this topic but has some limitations. Therefore localized level set has been proposed, which is able to consider intensity distribution in distance. This optimization cannot only increase accuracy of segmentation, but also repair faults resulting from incorrect initialization and inhomogeneous area. At last, most cases are involved in edge loss that leads to unfeasibility of almost segmentation methods. An edge compensation algorithm is presented to restore boundary part sheltered by tumor. The algorithm belongs to a low rank application for group of shapes similarity. In the experiment, statistics indicates strong superiority and stability in our method, while one without cannot be carried out in clinics at all.

There are some limitations. In some cases, air and tumor blend in Objects with blurring boundary cavity. Enormous gradient changes easily produce fake edge. Because of stochasticity, no one knows where and when it happens. So even localized or compensation idea could not work. We need more features like location of Objects with blurring boundary, tumor intensity to train our model. More, volume similarity or compensation will be another future work.

Acknowledgment

This research was supported by Science and technology project of State Grid (2019YF-35).

References

[1] KJ Cheng, YY Xu, ML Zhou, SH Zhou, and SQ Wang. Role of local allergic inflammation and staphylococcus aureus enterotoxins in chinese patients with chronic rhinoObjects with blurring boundaryitis with nasal polyps. The Journal of Laryngology & Otology, 131(8):707–713, 2017.

[2] Anneli Ahovuo-Saloranta, Ulla-Maija Rautakorpi, Oleg V Borisenko, He- lena Liira, John W Williams Jr, and Marjukka M¨akel¨a. Antibiotics for acute Objects with blurring boundaryitis in adults. Cochrane Database Syst Rev, 2(11), 2014.

[3] Do-Yeon Cho and Peter H Hwang. Results of endoscopic maxillary mega- antrostomy in recalcitrant Objects with blurring boundaryitis. American journal of rhinol- ogy, 22(6):658–662, 2008.
[4] Mustafa Kazkayasi, Yasemin Karadeniz, and Osman K Arikan. Anatomic variations of the sphenoid Objects with blurring boundary on computed tomography. Rhinology, 43(2):109–14, 2005.
[5] James A Stankiewicz. Complications of endoscopic intranasal ethmoidec- tomy. The Laryngoscope, 97(11):1270–1273, 1987.
[6] Arild Danielsen and Jan Olofsson. Endoscopic endonasal Objects with blurring boundary surgery: a review of 18 years of practice and long-term follow-up. European Archives of Oto-Rhino-Laryngology and Head & Neck, 263(12):1087–1098, 2006.
[7] Bernd Korves, Ludger Klimek, Hans-Martin Klein, and R M¨osges. Image- and model-based surgical planning in otolaryngology. The Journal of oto- laryngology, 24(5):265–270, 1995.
[8] Wolfgang Koele, Heinz Stammberger, Andreas Lackner, Pia Reittner, et al. Image guided surgery of Objects with blurring boundary and anterior skull base-five years experience with the instatrakR -system. Rhinology, 40(1):1–9, 2002.
[9] Arno Krueger, Christoph Kubisch, Bernhard Preim, and Gero Strauss. Objects with blurring boundary endoscopy-application of advanced gpu volume rendering for vir- tual endoscopy. iEEE transactions on visualization and computer graphics, 14(6):1491–1498, 2008.
[10] S Pirner, K Tingelhoff, I Wagner, R Westphal, M Rilk, FM Wahl, F Bootz, and Klaus WG Eichhorn. Ct-based manual segmentation and evaluation of Objects with blurring boundary. European archives of oto-rhino-laryngology, 266(4):507– 518, 2009.
[11] Paul A Yushkevich, Joseph Piven, Heather Cody Hazlett, Rachel Gimpel Smith, Sean Ho, James C Gee, and Guido Gerig. User-guided 3d active contour segmentation of anatomical structures: significantly improved effi- ciency and reliability. Neuroimage, 31(3):1116–1128, 2006.
[12] Leo Grady. Random walks for image segmentation. IEEE transactions on pattern analysis and machine intelligence, 28(11):1768–1783, 2006.
[13] Anthony Yezzi, Satyanad Kichenassamy, Arun Kumar, Peter Olver, and Allen Tannenbaum. A geometric snake model for segmentation of medical imagery. IEEE Transactions on medical imaging, 16(2):199–209, 1997.
[14] Chunming Li, Chenyang Xu, Changfeng Gui, and Martin D Fox. Level set evolution without re-initialization: a new variational formulation. In Com- puter Vision and Pattern Recognition, 2005. CVPR 2005. IEEE Computer Society Conference on, volume 1, pages 430–436. IEEE, 2005.
[15] I Lila Iznita, SA Vijanth, PA Venkatachalam, and SN Lee. Computerized segmentation of Objects with blurring boundary images. In Innovative Technologies in Intelligent Systems and Industrial Applications, 2009. CITISIA 2009, pages 125–128. IEEE, 2009.
[16] Maxime Descoteaux, Michel Audette, Kiyoyuki Chinzei, and Kaleem Sid- diqi. Bone enhancement filtering: Application to Objects with blurring boundary bone segmenta- tion and simulation of pituitary surgery. Medical Image Computing and Computer-Assisted Intervention–MICCAI 2005, pages 9–16, 2005.
[17] Anna Seo, SK Chung, Jun Lee, Jee-In Kim, and HyungSeok Kim. Semiau- tomatic segmentation of nasal airway based on collaborative environment. In Ubiquitous Virtual Reality (ISUVR), 2010 International Symposium on, pages 56–59. IEEE, 2010.
[18] T Heinone, P Dastidar, P Kauppinen, J Malmivuo, and H Eskola. Semi- automatic tool for segmentation and volumetric analysis of medical images. Medical and Biological Engineering and Computing, 36(3):291–296, 1998.

[19] Lila Iznita Izhar, Vijanth Sagayan Asirvadam, et al. Segmentation of Objects with blurring boundary images for grading of severity of Objects with blurring boundaryitis. In International Visual Infor- matics Conference, pages 202–212. Springer, 2009.
[20] Laura Fritz. Diffusion-based applications for interactive medical image seg- mentation. In Proceedings of the Central European Seminar on Computer Graphics (CESCG), volume 5, 2006. [21] Hongjian Shi, William C Scarfe, and Allan G Farman. Objects with blurring boundary 3d segmentation and reconstruction from cone beam ct data sets. International Journal of Computer Assisted Radiology and Surgery, 1(2):83–89, 2006.
[22] Zein Salah, Dirk Bartz, Florian Dammann, Erwin Schwaderer, Marcus Maassen, and Wolfgang Straßer. A fast and accurate approach for the seg- mentation of the paranasal Objects with blurring boundary. Bildverarbeitung fu¨r die Medizin 2005, pages 93–97, 2005.
[23] Nhat Linh Bui, Sim Heng Ong, and Kelvin Weng Chiong Foong. Automatic segmentation of the nasal cavity and Objects with blurring boundary from cone-beam ct images. International journal of computer assisted radiology and surgery, 10(8):1269–1277, 2015.
[24] Carsten Last, Simon Winkelbach, Friedrich Wahl, Klaus Eichhorn, and Friedrich Bootz. A model-based approach to the segmentation of nasal cavity and paranasal Objects with blurring boundary boundaries. Pattern Recognition, pages 333– 342, 2010.
[25] Robin Huang, Ang Li, Lei Bi, Changyang Li, Paul Young, Gregory King, David Dagan Feng, and Jinman Kim. A locally constrained statistical shape model for robust nasal cavity segmentation in computed tomography. In Biomedical Imaging (ISBI), 2016 IEEE 13th International Symposium on, pages 1334–1337. IEEE, 2016.
[26] Ayushi Sinhaa, Austin Reitera, Simon Leonarda, Masaru Ishiib, Gregory D Hagera, and Russell H Taylora. Simultaneous segmentation and correspon- dence improvement using statistical modes. In Proc. of SPIE Vol, volume 10133, pages 101331B–1, 2017.
[27] ED Roumanas, RD Nishimura, BK Davis, and J Beumer. Clinical evalua- tion of implants retaining edentulous maxillary obturator prostheses. Jour- nal of Prosthetic Dentistry, 77(2):184–190, 1997.
[28] Chunming Li, Chenyang Xu, Changfeng Gui, and Martin D Fox. Distance regularized level set evolution and its application to image segmentation. IEEE Transactions on Image Processing, 19(12):3243, 2010.
[29] Shawn Lankton and Allen Tannenbaum. Localizing region-based active contours. IEEE transactions on image processing, 17(11):2029–2039, 2008.
[30] Prateek Jain, Praneeth Netrapalli, and Sujay Sanghavi. Low-rank matrix completion using alternating minimization. In Proceedings of the forty-fifth annual ACM symposium on Theory of computing, pages 665–674. ACM, 2013.
[31] Hui Ji, Chaoqiang Liu, Zuowei Shen, and Yuhong Xu. Robust video de- noising using low rank matrix completion. In Computer Vision and Pattern Recognition (CVPR), 2010 IEEE Conference on, pages 1791–1798. IEEE, 2010.
[32] John Wright, Arvind Ganesh, Shankar Rao, Yigang Peng, and Yi Ma. Robust principal component analysis: Exact recovery of corrupted low- rank matrices via convex optimization. In Advances in neural information processing systems, pages 2080–2088, 2009.